Hindawi
Advances in Fuzzy Systems
Volume 2017, Article ID 4582948, 15 pages
https://doi.org/10.1155/2017/4582948

Research Article

Color Image Segmentation Using Fuzzy C-Regression Model

Min Chen[1] and Simone A. Ludwig[2]

[1]*State University of New York at New Paltz, New Paltz, NY, USA*
[2]*North Dakota State University, Fargo, ND, USA*

Correspondence should be addressed to Min Chen; chenm@newpaltz.edu

Received 9 November 2016; Revised 24 February 2017; Accepted 27 March 2017; Published 16 April 2017

Academic Editor: Katsuhiro Honda

Image segmentation is one important process in image analysis and computer vision and is a valuable tool that can be applied in fields of image processing, health care, remote sensing, and traffic image detection. Given the lack of prior knowledge of the ground truth, unsupervised learning techniques like clustering have been largely adopted. Fuzzy clustering has been widely studied and successfully applied in image segmentation. In situations such as limited spatial resolution, poor contrast, overlapping intensities, and noise and intensity inhomogeneities, fuzzy clustering can retain much more information than the hard clustering technique. Most fuzzy clustering algorithms have originated from fuzzy c-means (FCM) and have been successfully applied in image segmentation. However, the cluster prototype of the FCM method is hyperspherical or hyperellipsoidal. FCM may not provide the accurate partition in situations where data consists of arbitrary shapes. Therefore, a Fuzzy C-Regression Model (FCRM) using spatial information has been proposed whose prototype is hyperplaned and can be either linear or nonlinear allowing for better cluster partitioning. Thus, this paper implements FCRM and applies the algorithm to color segmentation using Berkeley's segmentation database. The results show that FCRM obtains more accurate results compared to other fuzzy clustering algorithms.

1. Introduction

Image segmentation [1, 2] is a necessary first process in image analysis and computer vision by correctly classifying the pixels of an image in decision-oriented applications. The essential goal of image segmentation is to partition an image into uniform and homogeneous attribute regions based on some likeness measure. Due to the variety and complexity of images, image segmentation is still a very challenging research topic. Various techniques have been introduced for object segmentation and feature extraction. Basically, segmentation approaches for images are based on the discontinuity and similarity of image intensity values [3]. Discontinuity is an approach which partitions an image based on abrupt changes. According to the predefined criteria, the similarity approach is based on partitioning an image into similar regions. Researchers have proposed a variety of techniques to tackle the challenging problem of image segmentation. In general, the image segmentation can be divided into four different categories [4]: thresholding, edge detection, region extraction, and clustering.

Thresholding [5] is one of the most popular approaches for image segmentation because of its simplicity. Image thresholding partitions an image based on gray levels or intensity values of the pixels. The objective of thresholding is to generate a binary representation of the image and classify each pixel into two categories, "dark" or "light." The challenge of thresholding is to find a correct gray level threshold, which can partition an image into a foreground and background.

Edge detection [6] is one of the most frequently used techniques in image segmentation. The image edges are detected and grouped into contours or surfaces to represent the boundaries of the objects. Edge detection aims to segment an image by finding and placing sharp discontinuities in gray level images. A very large amount of edge detection techniques are available. Each technique is designed to find certain types of edges.

Region extraction techniques [7] divide the entire image into subregions based on some criteria. These approaches make use of similarity in intensity, color, and texture to determine the partitioning of an image. Basically, there are two types of region-based methods [8]. One is a region

growing approach, which starts with a set of seed points and the regions grow by appending the neighboring pixels around the seed points with similar properties. The major challenges of this approach include how to select appropriate seed points and how to select suitable criteria during the growing process.

Markov Random Field-based (MRF) techniques [9] have recently been applied in image segmentation. The technique is based on the assumption that the true image can be viewed as a realization of a Markov random field with a distribution that can capture the spatial context of a scene [10]. The segmentation problem is an optimization problem that maximizes the marginal probabilities or posterior marginals by the given prior distribution of the true image and the observed noisy image. However, the MRF approaches are quite computationally expensive, and they require fairly accurate knowledge of the ground truth of the image.

Clustering is a process that can classify the objects or patterns into a predefined number of clusters such that the objects within a cluster have similar properties. In general, clustering methods can be divided into hierarchical and partitional approaches [11]. Hierarchical algorithms produce a nested series of partitions while partitional algorithms produce only one partition. Due to the fact that construction of a dendrogram is computationally expensive, partitional algorithms have gained more attention in image segmentation. Partitional algorithms include two main clustering strategies [12]: the hard clustering scheme and the fuzzy clustering scheme. The conventional hard clustering methods classify each object to only one cluster. As a consequence, the results are crisp. On the other hand, fuzzy clustering allows the objects to belong to two or more clusters with varying degrees of membership. Fuzzy clustering plays a significant role in various problems such as feature analysis, systems identification, and classification design [13]. Fuzzy clustering is more realistic than hard clustering due to the ability of handling impreciseness, uncertainty, and vagueness for real-world problems.

Fuzzy clustering has been widely studied and successfully applied in image segmentation. In situations such as limited spatial resolution, poor contrast, overlapping intensities, noise, and intensity inhomogeneities, fuzzy clustering can retain much more information than the hard clustering technique. Among the fuzzy clustering methods, fuzzy c-means (FCM) [14] is one of the most popular methods. FCM classifies an image into different clusters using an iterative method. The image is represented in various feature spaces, and FCM groups similar data points that are dependent on the distance of the pixels to the centroids in the feature domain.

The Fuzzy C-Regression Model (FCRM) was introduced by Bezdek et al. [15, 16]. Due to their excellent capability of describing complex systems in a human intuitive way, FCRM is capable of handling perceptual uncertainties and describing nonlinear system. FCRM, which can be viewed as an extension of FCM, divides the data set into a group of different regression models. Unlike FCM, the clustering prototype of FCRM is a hyperplane while FCM is hyperspherical.

However, because of the complexity of image segmentation and given that only partial prior knowledge is provided, the segmentation result would be poor if a supervised method was adopted. Thus, the unsupervised method is a better choice to solve such a problem. Although fuzzy theory has been employed in image segmentation, the application of FCRM to color images has been limited. In this paper, we explore the applicability and soundness of FCRM in color image segmentation. FCM can partition the fuzzy space efficiently; however it does not take linearity of the divided data into consideration. In contrast, the FCRM clustering algorithm with hyperplane-shaped cluster prototypes provides much more explanatory power, especially due to its multivariate nature.

In addition, the lack of spatial information is one of the problems of fuzzy-based clustering algorithms for image segmentation [17]. In order to overcome the image noise and other artifacts, we incorporate spatial information into FCRM. We adopt a similarity factor to incorporate local intensity and spatial information adapted from Chuang et al. [12]. Thus, our Fuzzy C-Regression Model clustering algorithm incorporates spatial information proposed to be applied to color image segmentation.

The remainder of the paper is organized as follows. Section 2 lists the related work regarding fuzzy image partitioning. Section 3 describes the Fuzzy C-Regression Model and the proposed approach applied to color image segmentation. Experimental results are presented in Section 4, and conclusions are drawn in Section 5.

2. Related Work

Related works with regard to the use of fuzzy theory in image segmentation include rule-based methods, fuzzy-geometrical methods, information theoretical methods, type II thresholding methods, and fuzzy clustering methods [18].

Past research related to rule-based methods uses fuzzy rules to determine a threshold in image segmentation. Images are considered as typical nonstationary signals. Fuzzy rule-based image processing techniques are applied to noise removal and edge extraction. A novel approach for enhancing the results of fuzzy clustering for solving image segmentation problems is introduced in [19]. A Sugeno-type rule-based system is developed to interact with the clustering result obtained by the FCM algorithm. In [20], an approach which combines an associative restoration algorithm with a fuzzy image enhancement technique is presented and is applied in electronic portal images in radiotherapy. However, fuzzy rule-based segmentation is sensitive to both the structure of the membership functions and parameter value selections. Thus, a generic fuzzy rule-based segmentation technique that tries to solve the problem of manual selection of the parameters of the fuzzy membership is introduced in [21]. This proposed technique is application-independent and incorporates spatial relationships between pixels. Fuzzy rules for image segmentation incorporating texture features (FRIST) are proposed in [22]. The fractal dimension and contrast features of texture are incorporated in FRIST by considering image domain specific information.

Fuzzy-geometrical methods [23], which focus on local image information, minimize or maximize fuzzy-geometrical

measures, such as compactness [24]. In [25], a new approach to multidimensional data clustering is described. The approach developed a "Radar" diagram shape matching methodology to accomplish the fuzzy geometric features technique for man-machine expert systems. A new quantitative index for image segmentation using the concept of homogeneity within regions is defined in [26]. The proposed index shows that the fuzzy geometry based thresholding algorithms produced a single stable threshold for a wide range of membership variations. A semisupervised FCM technique called GG-FCM is used to add geometrical information during clustering [27]. The approach is not only based on spectral information obtained by FCM, but also takes into consideration the geometrical relationship between neighboring pixels.

Related work on information theoretical methods uses measurements such as fuzzy entropy, index of fuzziness, and fuzzy divergence to minimize or maximize fuzzy information. In [28], a new measure called divergence between two fuzzy sets is introduced and a tailored version of the probability measure of a fuzzy event is also used for image segmentation. A complete method can be viewed as a weighted moving average technique; grayness ambiguity being the weights is introduced in [29]. An image thresholding approach based on the index of nonfuzziness maximization of the 2D grayscale histogram is introduced in [30] and has shown that the approach is more robust when applied to noisy images.

Type II thresholding methods interpret image information as Type II fuzzy sets. These methods use information theoretical measures to locate a global threshold [18]. In [31], an evolving fuzzy classifier approach that is able to adapt and evolve at an on-line machine vision system is introduced. In [32], new modified thresholding measures for MRI brain images using type 1 and type 2 fuzzy sets are presented. An interval type 2 (IT2) fuzzy entropy based approach is used to compute optimum thresholds for multistage gray scale image segmentation in [33]. An automatic leukocyte segmentation using intuitionistic fuzzy and interval Type II fuzzy set theory in pathological blood cell images is presented in [34]. The use of intuitionistic fuzzy set and interval Type II fuzzy set can consider more uncertainties and different types of uncertainty as compared to basic fuzzy set theory.

Fuzzy clustering methods classify all image pixels into different segments. Up to now, FCM is one of the most commonly used methods in image segmentation, and there have been many variants of fuzzy clustering algorithms that originated from FCM. A modified fuzzy c-means clustering algorithm for MR brain image segmentation is introduced in [35]. The proposed algorithm extracts a scalar feature value from the neighborhood of each pixel. It converges faster than standard FCM in the case of mixed noise. An improved FCM algorithm for image segmentation, which introduces a tradeoff weighted fuzzy factor and a kernel metric, is introduced in [36]. The proposed algorithm using a tradeoff weighted fuzzy factor can accurately estimate the damping extent of neighboring pixels. FCM is sensitive to noise in the image since it ignores the spatial information contained in the pixels. A novel fuzzy clustering algorithm with nonlocal adaptive spatial constraints is presented in [37]. The approach uses an adaptive spatial parameter for each pixel to guide the noisy image segmentation process. Ji et al. [38] proposed the weighted image patch-based FCM algorithm for image segmentation. The algorithm improves its robustness to noise by incorporating local spatial information embedded within the segmentation process. In color image segmentation, it is difficult to analyze the image on all of its colors. Soft computing techniques, namely, FCM, possibilistic fuzzy c-means, and competitive neural networks, have been used to group likely colors [39]. A novel initialization scheme to determine the cluster number and obtain the initial cluster centers for the FCM algorithm to segment color images is introduced in [40]. The initialization scheme called hierarchical approach is proposed to integrate the splitting and merging techniques to obtain the initialization condition for FCM. The proposed algorithm can obtain the reasonable cluster number for any kind of color images. An Adaptive Neuro-Fuzzy Color Image Segmentation (ANFCIS) approach is presented in [41].

A hybrid image segmentation approach using discerner clusters and histogram thresholding is proposed in [42]. The approach applies the standard FCM clustering algorithm to the frequencies of the smoothed histogram and, thus, the histogram with the maximum frequency is used to discern clusters to the gray level image. This approach overcomes some of the limitations of traditional thresholding methods in particular the definition of the initial threshold cut point.

In [43], an image segmentation algorithms are presented that are based on a hybrid combination of differential evolution, particle swarm optimization, and fuzzy c-means clustering. The use of differential evolution and particle swarm optimization solves the problem of the influence of the initial cluster centers on the fuzzy c-means algorithm. The experiments showed that the proposed algorithm has a strong antinoise ability and thus can improve FCM achieving better image segmentation results.

In the medical domain, a fuzzy c-means algorithm [44] with wavelet filtration is proposed to address the magnetic resonance image segmentation problem. The idea is to use the image noise feature estimation that is composed of preliminary coefficient classification and wavelet domain indicators to filter for balancing the preservation of relevant details against the noise reduction created. In addition, the filter is merged with the fuzzy c-means algorithm as part of the membership function. Thus, the proposed approach does not only exploit useful spatial information but also minimize dynamically the clustering errors that are caused by noise in medical images.

In [45], an approach is presented that overcomes the noise sensitiveness of the conventional fuzzy c-means clustering algorithm. The proposed approach extends the fuzzy c-means algorithm by proposing a modified objective function. The modified objective function includes a penalty term that takes the influence of the neighboring pixels on the center pixels into consideration. Thus, the penalty term acts as a regularizer that was inspired from the neighborhood expectation maximization algorithm. The experimental results both on synthetic and real images demonstrate the effectiveness and robustness of the proposed algorithm.

Most fuzzy clustering algorithms have originated from FCM and have been successfully applied in image segmentation. However, the cluster prototype of the FCM method is either hyperspherical or hyperellipsoidal. FCM may not provide an accurate partition in situations where data consists of arbitrary shapes. On the other hand, the prototype of the FCRM method is hyperplaned and can be either linear or nonlinear. Cai et al. [17] proposed a generalized FCM algorithm that adopts a similarity factor to incorporate local intensity and spatial information. In addition, [17] proposed another spatial FCM algorithm in which spatial information can be incorporated into fuzzy membership functions directly. Thus, this paper implements the FCRM method by adopting the approach in [12] applied to color segmentation of images. This is the first work that applies the FCRM method incorporating spatial information in color segmentation. The results show that FCRM obtains more accurate results compared to other fuzzy clustering algorithms. Furthermore, besides presenting FCRM's competitiveness with respect to the other fuzzy clustering algorithms, FCRM's practical value is demonstrated when applied to the task of color image segmentation.

3. Proposed Approach

This section first describes the color space that is used for the proposed color segmentation approach, followed by the proposed Fuzzy C-Regression Model clustering approach, and the cluster validation techniques used for the evaluation of the approach.

*3.1. CIE-L*A*B* Color Space.* Color space is a way of representing color information based on certain criteria. Color perceived by human-beings combines primary colors which are R (red), G (green), and B (blue). By using either linear or nonlinear transformations, other kinds of color representations or spaces can be derived from the R, G, and B representation [46]. Color spaces like RGB, HSV (Hue-Saturation-Value) [47], and CIE-L*A*B* [48] have been successfully applied in color image segmentation. In this paper, the CIE-L*A*B* color space is selected and explored in color image segmentation. CIE-L*A*B* is a color-opponent space with dimensions L, A, and B. L denotes lightness, and A and B are the color-opponent dimensions. The CIE-L*A*B* color space includes all perceivable colors and it is device-independent, which means that the colors are independent of the device they are displayed on. Specifically, L with a range between 0 and 100 represents the lightness; 0 represents the darkest black, while 100 represents the brightest white. The red-green opponent colors are represented by the A axis. The yellow-blue opponent colors are represented by the B axis. Both A and B have negative and positive values. Negative values of A represent green colors while positive values of A represent red colors. Similarly, negative values of B represent yellow colors, and positive values of B represent blue colors. The range of A and B can be either ±100 or ±128 depending on the specific implementation.

3.2. Fuzzy C-Regression Model Clustering. The Fuzzy C-Regression Model clustering algorithm has become popular the past few years since the resulting model can explain and describe complex systems in a human intuitive way. Takagi and Sugeno [49] introduced the well-known T-S fuzzy model to describe a complicated nonlinear system. A T-S fuzzy model consists of a set of fuzzy rules, each describing a local input-output relation as follows.

Rule i. IF x_1 is A_1^i and ... and x_M is A_M^i then

$$y_i = \theta_i^0 + \theta_i^1 x_1 + \cdots + \theta_i^M x_M, \tag{1}$$

where $X = [x_1, \ldots, x_M]$ is the system input, M is the dimension of input vector, $i = 1, \ldots, c$ is the number of fuzzy rules, y_i is the ith output, and θ_i^M is the consequent parameter of the ith output.

Fuzzy clustering as one of the soft computing techniques can allow the data points to belong to more than one cluster. Fuzzy clustering has been successfully applied in data analysis, pattern recognition, and image segmentation [39]. The shell clustering algorithms such as FCM have been largely applied in image segmentation. The shell clustering algorithms detect the special geometrical shapes like circles, rectangles, hyperbolas, and ellipses using the Euclidean distance measure [39]. Unlike the shell clustering algorithms, the Fuzzy C-Regression Model (FCRM) [15, 16], which was introduced by Bezdek et al. in 1993, assumes that the data is drawn from c different models instead of one single model. The c different models represent c hyperplane-shaped clusters. The FCRM clustering algorithm is an affine T-S model with linear prototypes.

Let $S = (X(k), y_k)$, $k = 1, \ldots, N$ be a set of input-output sample data pairs, where N is the number of patterns, $X_k = [x_1, x_2, \ldots, x_M] \subset R^m$ is the kth input data vector, M is the number of input variables, y is output vector, y_k is the kth desired output for x_k, and $\theta_i = [b_i^0, b_i^1, \ldots, b_i^M]$ is the parameter vector of the corresponding local linear model. Assume that the data pairs in S are drawn from c different fuzzy models. The ith hyperplane-shaped cluster of the kth input can be denoted as follows:

$$y_k^i = b_i^0 + b_i^1 x_{k1} + \cdots + b_i^M x_{kM} = [x_k, 1] \cdot \theta_i^T, \quad i = 1, \ldots, c. \tag{2}$$

The cost function of the FCRM clustering algorithm is defined as follows:

$$J(S; U, \theta) = \sum_{k=1}^{N} \sum_{i=1}^{c} (\mu_{ik}^m) E_{ik}^2(\theta_i), \tag{3}$$

where the distance $E_{ik}(\theta_i)$ is defined as

$$E_{ik}(\theta_i) = \left| y_k - [x_k 1] \cdot \theta_i^T \right|. \tag{4}$$

m is fuzzy weighted exponent and μ_{ik} is the membership degree of x_k to the ith hyperplane-shaped cluster. The membership values μ_{ik} have to satisfy the following constraints:

$$\mu_{ik} \in [0 \quad 1], \quad i = 1, 2, \ldots, c; \; k = 1, 2, \ldots, N,$$
$$\sum_{i=1}^{c} \mu_{ik} = 1, \quad k = 1, 2, \ldots, N. \tag{5}$$

The Fuzzy C-Regression Model clustering algorithm is summarized as follows [15, 16]. Given data S, set $m > 1$ and specify the regression models, choose an error measure and a termination threshold $\epsilon > 0$, and initialize $U^{(0)}$ randomly.

(1) Repeat for $l = 1, 2, \ldots, \infty$

(2) Calculate the c model parameters $\theta_i^{(l)}$, which globally minimizes the cost function

(3) Update $U^{(l)}$ with $E_{ik}(\theta_i^{(l)})$ to satisfy

$$U_{ik}^{(l)} = \begin{cases} \left[\sum_{j=1}^{c} \left(\dfrac{E_{ik}}{E_{jk}} \right)^{2/(m-1)} \right]^{-1}, & \text{if } E_{ik} > 0 \text{ for } 1 \le i \le c, \\ 0, & \text{otherwise.} \end{cases} \tag{6}$$

(4) Until $\|U^{(l)} - U^{(l-1)}\| \le \epsilon$, then stop; otherwise, $l = l+1$ and return to Step (2).

It is a common problem that a noisy pixel is wrongly classified due to its abnormal feature data. In this paper, unlike the standard FCRM clustering algorithm, we adopt a similarity factor from [12] in which spatial information can be incorporated into fuzzy membership functions directly using

$$\mu' = \frac{\mu_{ik}^{p} h_{ik}^{q}}{\sum_{l=1}^{C} \mu_{lk}^{p} h_{lk}^{q}}, \tag{7}$$

where p and q are parameters which can control the respective contribution. h_{mn} includes spatial information and is calculated by

$$h_{ik} = \sum_{i \in M_i} \mu_{ik}, \tag{8}$$

where M_i denotes a local window centered around the image pixel i. The only difference between the standard FCRM and the proposed FCRM is the process of updating the membership function. The u_{ik} are updated as usual according to (6). In addition, the membership information of each pixel is mapped to the spatial domain, and the spatial function is computed using (8). The FCRM iteration proceeds with the new membership that is incorporated within the spatial function. The conventional FCRM generates spurious blobs due to the noisy pixels. In this proposed approach, the spatial function modifies the membership function (see (6)) of a pixel according to the membership statistics of its neighborhood. Membership functions of the neighbors centered on a pixel in the spatial domain are listed to estimate the cluster distribution statistics. These statistics are transformed into a weighting function which are then incorporated into (7). This neighboring effect reduces the number of spurious blobs and biases the solution toward piecewise homogeneous labeling.

Other variations of spatial function are available. One example can be expressed as follows:

$$h_{ik} = \sum_{i \in M_i} g_{ik}, \tag{9}$$

where

$$g_{ik} = \begin{cases} 1, & \text{if } \mu_{ik} \ge \mu_{jk} \text{ for } j = 1, \ldots, c, \\ 0, & \text{otherwise.} \end{cases} \tag{10}$$

However, this expression of membership has less fuzziness than (8) and causes a loss in the details. Moreover, the spatial function can be incorporated with the proposed FCRM technique without a great deal of modifications. The spatial function (8) is estimated at each iteration and is incorporated into the membership function. The proposed FCRM technique is less sensitive than the conventional FCRM to noise due to the incorporation of spatial information.

The procedures of the proposed approach using FCRM in color image segmentation can be summarized into four phases: image preprocessing, FCRM clustering, image reconstruction, and evaluation.

Image Preprocessing. The images are converted from the RGB color space to the CIE-L*A*B* color space during this phase. The *A and *B values, which are extracted from the RGB color space, serve as the color markers in the A*B* space.

FCRM Clustering. The A*B* space image data is given, and the number of clusters is fixed during this phase. A FCRM clustering algorithm is used to partition the given data into a fixed number of clusters.

Image Reconstruction. The cluster results from the FCRM clustering step are used to reconstruct the image in grayscale level during this phase.

Evaluation. The performance of the cluster results is evaluated using the results from the FCRM clustering process. The performance of the proposed algorithm is evaluated with three validity indices (explained in the following section). In addition, two other measures commonly used to access FCRM are calculated during this phase.

3.3. Clustering Validation Techniques. The aim of clustering validation is to evaluate the clustering results by finding the best partition that fits the underlying data best. Thus, cluster validity is used to quantitatively evaluate the results of clustering algorithms. Compactness and separation are two widely considered criteria for measuring the quality of the partitioning of a data set into different numbers of clusters. Conventional approaches use an iterative approach by choosing different input values, and they select the best validity measure to determine the "optimum" number of clusters. A list of validity indices for fuzzy clustering is listed below.

3.3.1. Partition Coefficient (PC) Index. The Partition Coefficient (PC) is defined as follows [15]:

$$\mathrm{PC} = \frac{1}{n}\sum_{i=1}^{n}\sum_{j=1}^{c} u_{ij}^{2}; \tag{11}$$

PC obtains its maximum value when the cluster structure is optimal.

3.3.2. Partition Entropy (PE) Index. The Partition Entropy (PE) was defined as follows [50]:

$$\mathrm{PE} = -\frac{1}{n}\sum_{i=1}^{n}\sum_{j=1}^{c} u_{ij}\log_{b}\left(u_{ij}\right), \tag{12}$$

where b is the logarithmic base. PE achieves its minimum value when the cluster structure is optimal.

3.3.3. Modified Partition Coefficient (MPC) Index. Modification of the PC index, which can reduce the monotonic tendency, was proposed by Dave in 1996 [51].

$$\mathrm{MPC} = 1 - \frac{c}{c-1}\left(1 - \mathrm{PC}\right), \tag{13}$$

where c is the number of clusters. An optimal cluster number is found by maximizing MPC to produce the best clustering performance for a data set.

4. Experiments and Results

This section describes the experimental setup used and the results obtained by the experiments conducted. In particular, a comparison of the cluster performance in the ${}^{*}\mathrm{A}{}^{*}\mathrm{B}$ space is conducted applying FCM, GK (Gustafson-Kessel), and the proposed FCRM approach. Then, the different validity indices are compared with FCM and GK, followed by a comparison of the mean square error and the peak-signal-to-noise ratio. The last subsection shows the segmentation results.

4.1. Experimental Setup. The experiments are implemented and evaluated on an ASUS desktop (Intel(R) Dual Core I3 CPU @3.07 GHz, 3.07 GHz) MATLAB Version 7.13. In order to evaluate the performance of the proposed method, the algorithm has been tested using synthetic data and real-world data for color image segmentation. In addition, the two other fuzzy clustering algorithms, FCM and Gustafson-Kessel (GK), have been used to compare FCRM with FCM and GK . Table 1 lists the required parameters used when running FCM, GK, Fuzzy Clustering Using Automatic Particle Swarm Optimization (FPSO) [52], and FCRM.

4.1.1. Datasets. The experiments are conducted on synthetic data sets which were generated using MATLAB and a number of datasets taken from the Berkeley Segmentation Database [53] for color image segmentation. The datasets are described in Table 2.

Table 1: FCM, GK, FPSO, and FCRM algorithms with the same parameters and values.

Parameter	Value
p	1
q	1
$\lvert U^{l} - U^{l-1}\rvert < \epsilon$	10^{-3}
Fuzzification coefficient (m)	2
Maximum number of clusters	10

Table 2: Datasets used for the experiments.

Data Set	Dimensions	Instances	Classes
Synthetic data			
Pinwheel2	2	1000	2
Pinwheel3	3	1000	3
Pinwheel4	4	1000	4
Image data from BSD			
IMG1–15			

Table 3: Average execution time (in seconds) for FCM, GK, FPSO, and FCRM with fixed clusters number.

Data sets	FCM	GK	FPSO	FCRM
Pinwheel2	2.14	2.36	15.32	2.45
Pinwheel3	2.81	3.12	21.45	3.57
Pinwheel4	3.22	3.27	31.17	4.11

4.2. Experimental Study

4.2.1. Use of Synthetic Data. In order to investigate the clustering performance with different numbers of clusters, we use a synthetic data set, named pinwheel, to test the clustering performance using FCM, Gustafson-Kessel (GK), Fuzzy Clustering Using Automatic Particle Swarm Optimization (FPSO), and our proposed algorithm (FPSO). The pinwheel data set is a 2-, 3-, or 4-dimensional data set with 1000 records. The performance of the results is listed in Table 3 . The FPSO [52] is a method which can automatically determine the optimal number of clusters using a threshold vector that is added to the particle. The algorithm starts by partitioning the data set randomly within a preset maximum number of clusters in order to overcome the fuzzy c-means shortcoming of the predefined cluster count. The three pinwheel data sets are tested 10 times and the average execution times in seconds are calculated, respectively. The maximum number of clusters for FPSO is predefined as 5.

However, due to the slow convergence and the stochastic nature of the PSO algorithm, the prediction results of a single run fluctuates and it is thus hard to make predictions. Unlike FCM, GK, and FCRM, FPSO needs to be tested repeatedly in order to find the optimal solution. In addition, the maximum number of clusters is predefined for FPSO, and the recursive increase of the number of clusters is computationally expensive. As shown from Table 3, FPSO requires a lot more time for execution. Thus, a comparison

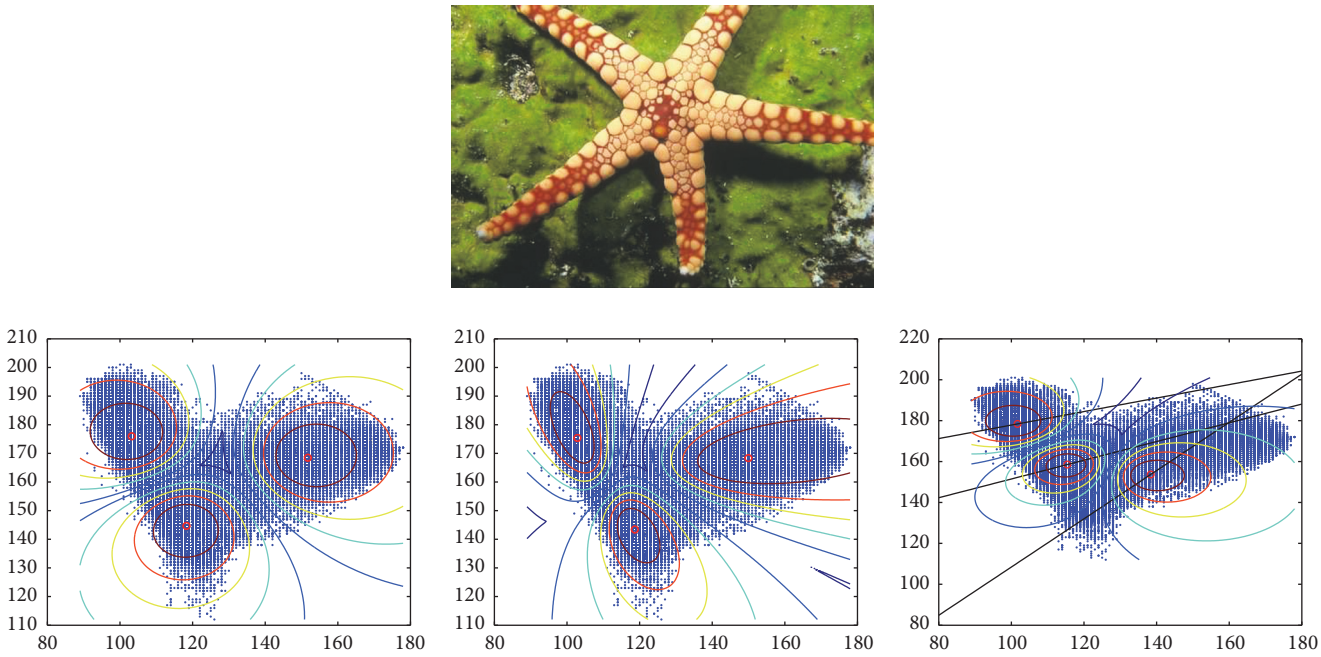

FIGURE 1: Original image, FCM, GK, and FCRM with $c = 3$ in $^*a^*b$ color space.

of the cluster performance in the $^*A^*B$ space is conducted applying FCM, GK, and the proposed FCRM approach.

4.2.2. Use of Real-World Data

(1) Comparison of Cluster Performance in $^*A^*B$ Space. There are many different types and applications in color spaces [54]. The main difference between these color models is whether the model is device-dependent or device-independent. RGB and HVS [47] are device-dependent while CIE-L*A*B* is device-independent. The device-dependent spaces can express color relative to some other reference space. The color elements and their response to the individual R, G, and B levels vary from manufacturer to manufacturer, or even in the same device over time. Thus, different devices detect or reproduce a given RGB value differently. On the other hand, CIE-L*A*B* is device-independent. The LAB color spaces express color in absolute terms which can be served as universal reference colors. In addition, CIE-L*A*B* can produce a color space that is more perceptually linear than other color spaces. Thus, the use of CIE-L*A*B* color is more suitable for the proposed algorithm due to the linearity of FCRM.

In order to test the cluster performance of FCM, GK, and FCRM, we firstly use IMG1 with $c = 3$ tested and the performance is displayed in Figure 1. The top figure is the original image. The remaining three figures show the cluster centers in CIE-L*A*B* color space using FCM, GK, and FCRM, respectively. The three hyperspherical centers obtained by FCM and GK and the three hyperplane-shaped clusters obtained by FCRM are listed in Table 4.

As shown in Figure 1, the proposed FCRM partitions the image into 3 hyperplaned clusters, while FCM and GK group the image into hyperspherical clusters, respectively. The FCRM method provides better results of the constructed fuzzy model as compared to FCM and GK.

(2) Comparison Using Different Validity Indices. Table 5 lists the cluster performance of FCM, GK, and FCRM using validity indices PC, PE, and MPC, respectively. As shown in the table, the values in bold denote the best values obtained from the three different validity indices. In most cases, FCRM has the better performance compared to FCM and GK in terms of objective values.

In addition, the best cluster numbers of FCM, GK, and FCRM obtained by using PC, PE, and MPC are listed in Table 6. In most cases we can see that the best cluster number is 2 when using PC, PE, and MPC as the validity index.

The one-tailed t-test with a significance level of 0.10 is performed on the data set of any difference in the measures. The null hypothesis is applied. The statistical results are listed in Table 7. The results indicate that PC and PE of the proposed FCRM are significant greater (smaller value) than conventional FCM and GK. MPC of the proposed is significantly greater than FCM. However, MPC of GK is significant greater than FCRM. It is understandable that MPC measures the compactness in the feature domain. The partition achieved by GK is estimated by maximizing the MPC in the feature domain. On the other hand, the partition of the proposed FCRM is modified by the spatial distribution which causes deterioration of the compactness in the feature domain. Hence, MPC is decreased subsequently.

(3) Comparison with MSE and PSNR. Mean Square Error (MSE) [55] and Peak Signal-to-Noise Ratio (PSNR) [56] are used as the performance indices in fuzzy modeling, which are defined as follows:

Table 4: Centroids of FCM, GK, and FCRM with $c = 3$ in $^*a^*b$ color space.

	FCM	GK	FCRM
Cluster 1	(151.73, 168.49)	(122.26, 146.33)	$y_1 = 0.3297 \times (x - 80) + 171.243$
Cluster 2	(103.24, 175.97)	(114.69, 132.16)	$y_2 = 1.1788 \times (x - 101.34) + 110$
Cluster 3	(118.33, 144.69)	(135.42, 158.93)	$y_3 = 0.4578 \times (x - 80) + 142.315$

Table 5: FCM, GK, and FCRM using three different indices (PC, PE, and MPC).

	PC			PE			MPC		
	FCM	GK	FCRM	FCM	GK	FCRM	FCM	GK	FCRM
IMG1	0.77	0.77	**0.81**	0.44	0.44	**0.35**	0.65	0.65	**0.71**
IMG2	0.79	**0.82**	0.78	0.38	**0.34**	0.39	0.68	**0.73**	0.68
IMG3	0.72	0.69	**0.78**	0.50	0.55	**0.40**	0.58	0.53	**0.67**
IMG4	0.68	0.70	**0.80**	0.57	0.53	**0.35**	0.51	0.54	**0.70**
IMG5	0.67	0.68	**0.80**	0.58	0.56	**0.36**	0.51	0.52	**0.70**
IMG6	0.66	**0.83**	0.81	0.56	**0.32**	0.35	0.50	**0.75**	0.71
IMG7	**0.88**	0.83	**0.88**	0.23	0.30	**0.22**	0.81	0.75	**0.83**
IMG8	0.77	0.77	**0.82**	0.42	0.41	**0.33**	0.66	0.65	**0.73**
IMG9	0.74	0.75	**0.79**	0.46	0.45	**0.38**	0.61	0.63	**0.68**
IMG10	0.69	0.72	**0.78**	0.55	0.48	**0.39**	0.54	0.58	**0.67**
IMG11	0.75	**0.77**	**0.77**	0.46	**0.40**	0.41	0.62	**0.66**	**0.66**
IMG12	0.75	0.74	**0.80**	0.46	0.46	**0.37**	0.62	0.61	**0.69**
IMG13	0.75	0.74	**0.83**	0.45	0.47	**0.31**	0.63	0.62	**0.74**
IMG14	0.85	0.84	**0.87**	0.28	0.30	**0.25**	0.77	0.76	**0.80**
IMG15	0.65	0.66	**0.78**	0.62	0.60	**0.40**	0.48	0.48	**0.67**

Table 6: Best cluster number of FCM, GK, and FCRM using PC, PE, and MPC.

	PC			PE			MPC		
	FCM	GK	FCRM	FCM	GK	FCRM	FCM	GK	FCRM
MG1	3	2	3	2	2	2	2	2	2
MG2	2	2	2	2	2	3	2	2	7
IMG3	2	2	2	2	2	2	2	2	2
IMG4	2	2	2	10	10	10	2	2	10
IMG5	2	2	2	2	2	2	2	2	2
IMG6	2	2	2	3	3	3	2	2	2
IMG7	2	2	2	2	2	2	2	2	2
IMG8	2	2	2	3	2	3	2	2	3
IMG9	2	2	2	2	2	2	2	2	2
IMG10	2	2	5	2	2	2	2	2	2
IMG11	2	2	4	2	2	3	2	2	4
IMG12	2	2	2	2	2	2	2	2	2
IMG13	2	2	5	2	2	3	2	2	3
IMG14	2	2	2	2	2	10	2	2	2
IMG15	2	2	2	2	2	2	2	2	2

Table 7: Statistical results of the one-tailed t-test ($\alpha = 0.10$) on the differences using PC, PE, and MPC.

Validity index	X versus Y	SD (standard deviation)	T Score	p value
PC	FCM v.s. FCRM	0.0479	1.3915	$p = 0.0922 < 0.10$
	GK v.s. FCRM	0.0359	1.6875	$p = 0.0561 < 0.10$
PE	FCM v.s. FCRM	0.0763	1.5022	$p = 0.0769 < 0.10$
	GK v.s. FCRM	0.0612	1.6666	$p = 0.0582 < 0.10$
MPC	FCM v.s. FCRM	0.1290	2.1714	$p = 0.0232 < 0.10$
	GK v.s. FCRM	0.0615	0.6399	$p = 0.2659 > 0.10$

Table 8: MSE ($\times 10^3$) using FCM with different cluster number.

	$c = 2$	3	4	5	6	7	8	9	10
IMG1	5.92	4.15	3.22	2.58	2.32	2.07	1.67	1.50	1.27
IMG2	3.74	2.60	1.89	1.64	1.48	1.31	1.06	0.96	0.81
IMG3	7.99	5.42	4.05	3.21	2.89	2.57	2.08	1.87	1.58
IMG4	10.38	7.02	5.21	4.24	3.82	3.40	2.75	2.47	2.09
IMG5	3.91	2.72	2.11	1.62	1.46	1.30	1.05	0.94	0.80
IMG6	4.84	4.10	3.62	2.84	2.56	2.27	1.84	1.66	1.40
IMG7	4.13	2.71	2.65	2.49	2.24	1.99	1.61	1.45	1.23
IMG8	4.78	3.44	2.49	2.04	1.84	1.63	1.32	1.19	1.00
IMG9	9.84	6.64	5.04	4.03	3.63	3.23	2.61	2.35	1.98
IMG10	9.91	6.93	5.58	4.61	4.15	3.69	2.99	2.69	2.27
IMG11	9.31	6.18	4.71	3.79	3.41	3.04	2.46	2.21	1.87
IMG12	7.90	6.11	4.33	4.11	3.70	3.29	2.66	2.40	2.02
IMG13	6.42	4.51	3.44	2.72	2.45	2.18	1.76	1.59	1.34
IMG14	7.31	4.94	3.69	2.44	2.20	1.95	1.58	1.42	1.20
IMG15	5.82	4.03	2.99	2.49	2.24	1.99	1.61	1.45	1.23

Table 9: MSE ($\times 10^3$) using GK with different cluster number.

	$c = 2$	3	4	5	6	7	8	9	10
IMG1	5.83	4.22	3.13	2.56	2.30	2.05	1.66	1.49	1.26
IMG2	3.73	2.60	1.91	1.62	1.46	1.30	1.05	0.94	0.80
IMG3	7.92	5.44	4.04	3.19	2.87	2.56	2.07	1.86	1.57
IMG4	10.51	7.01	5.13	4.23	3.81	3.39	2.74	2.47	2.08
IMG5	3.90	2.63	2.03	1.59	1.43	1.27	1.03	0.93	0.78
IMG6	5.20	5.20	3.96	3.21	2.89	2.57	2.08	1.87	1.58
IMG7	4.10	2.69	2.92	2.48	2.23	1.99	1.61	1.45	1.22
IMG8	5.02	3.43	2.54	1.98	1.78	1.59	1.28	1.15	0.98
IMG9	9.81	6.62	5.01	3.99	3.59	3.20	2.59	2.33	1.96
IMG10	9.83	7.77	5.72	4.73	4.26	3.79	3.07	2.76	2.33
IMG11	9.32	6.17	4.68	3.78	3.40	3.03	2.45	2.20	1.86
IMG12	8.01	6.22	4.74	3.84	3.46	3.08	2.49	2.24	1.89
IMG13	6.87	4.22	3.42	2.69	2.42	2.15	1.74	1.57	1.32
IMG14	7.31	4.93	3.66	2.92	2.63	2.34	1.89	1.70	1.44
IMG15	5.89	4.04	2.96	2.52	2.27	2.02	1.63	1.47	1.24

$$\text{MSE} = \frac{1}{n}\sum_{k=1}^{n}\left(y_k - \widehat{y}_k\right)^2,$$
$$\text{PSNR} = \frac{10 \times \log\left(255 \times 255/\text{MSE}\right)}{\log\left(10\right)}. \tag{14}$$

Tables 8, 9, and 10 list the MSE of the 15 images using FCM, GK, and FCRM, respectively. Tables 11, 12, and 13 list the PSNR of the 15 images obtained from FCM, GK, and FCRM, respectively. The MSE and PSNR are measured with a cluster number varying from 2 to 10. The results show that FCM, GK, and FCRM show the same trend regarding MSE and PSNR. As the number of clusters increases, the values of MSE decrease, and the values of PSNR increase for the 15 tested images. In addition, FCRM has a better performance than FCM and GK in terms of both MSE and PSNR. Therefore, FCRM has less partition errors and a more compact representation than FCM and GK.

(4) Comparison on Segmentation Results. The cluster results are used to reconstruct the image in grayscale level as shown in Figures 2 and 3 with $c = 2$ (see Table 4 which shows that the optimal cluster number is 2). As shown in the figures, the FCM, GK, and FCRM can segment the images clearly.

5. Conclusion

Most fuzzy clustering algorithms have been successfully applied in image segmentation. However, the disadvantage they have is that the cluster prototype of FCM (fuzzy c-means) is either hyperspherical or hyperellipsoidal. Therefore, FCM may not provide accurate partitioning in circumstances where data is better modeled by arbitrary shapes. Thus, a Fuzzy C-Regression Model (FCRM) clustering algorithm has been introduced whose prototype is hyperplaned

Table 10: MSE ($\times 10^3$) using FCRM with different cluster number.

	$c = 2$	3	4	5	6	7	8	9	10
IMG1	5.73	4.01	3.07	2.53	2.28	2.03	1.64	1.48	1.25
IMG2	3.71	2.52	1.92	1.55	1.40	1.24	1.00	0.90	0.76
IMG3	7.80	5.43	3.97	3.16	2.84	2.53	2.05	1.84	1.56
IMG4	8.25	6.23	5.01	4.21	3.79	3.37	2.73	2.46	2.07
IMG5	3.89	2.60	1.99	1.58	1.42	1.27	1.02	0.92	0.78
IMG6	4.83	4.40	3.33	2.83	2.55	2.27	1.83	1.65	1.39
IMG7	3.98	2.68	2.61	2.45	2.21	1.96	1.59	1.43	1.21
IMG8	4.98	3.49	2.48	1.96	1.76	1.57	1.27	1.14	0.97
IMG9	9.77	6.58	4.96	3.98	3.58	3.19	2.58	2.32	1.96
IMG10	9.51	7.62	5.54	4.42	3.98	3.54	2.86	2.58	2.18
IMG11	9.30	6.10	4.65	3.77	3.39	3.02	2.44	2.20	1.86
IMG12	7.85	5.52	5.21	4.21	3.79	3.37	2.73	2.46	2.07
IMG13	6.84	4.21	3.21	2.65	2.39	2.12	1.72	1.55	1.31
IMG14	7.30	4.62	3.65	2.43	2.19	1.95	1.57	1.42	1.20
IMG15	5.71	3.93	2.81	2.48	2.23	1.99	1.61	1.45	1.22

Table 11: PSNR using FCM with different cluster number.

	$c = 2$	3	4	5	6	7	8	9	10
IMG1	10.41	11.95	13.05	14.01	14.47	14.98	15.90	16.36	17.09
IMG2	12.40	13.98	15.37	15.98	16.44	16.95	17.87	18.32	19.06
IMG3	9.11	10.79	12.06	13.07	13.52	14.03	14.95	15.41	16.14
IMG4	7.97	9.67	10.96	11.86	12.31	12.82	13.74	14.20	14.93
IMG5	12.21	13.79	14.89	16.04	16.49	17.00	17.92	18.38	19.11
IMG6	11.28	12.00	12.54	13.60	14.06	14.56	15.48	15.94	16.67
IMG7	11.97	13.80	13.90	14.17	14.63	15.13	16.05	16.51	17.24
IMG8	11.34	12.77	14.17	15.03	15.49	16.00	16.92	17.38	18.11
IMG9	8.20	9.91	11.11	12.08	12.54	13.04	13.96	14.42	15.15
IMG10	8.17	9.72	10.66	11.49	11.95	12.46	13.38	13.84	14.57
IMG11	8.44	10.22	11.40	12.34	12.80	13.31	14.23	14.69	15.42
IMG12	9.15	10.27	11.77	11.99	12.45	12.96	13.88	14.33	15.07
IMG13	10.06	11.59	12.77	13.79	14.24	14.75	15.67	16.13	16.86
IMG14	9.49	11.19	12.46	14.26	14.71	15.22	16.14	16.60	17.33
IMG15	10.48	12.08	13.37	14.17	14.63	15.13	16.05	16.51	17.24

and can either be linear or nonlinear. FCRM is an affine T-S model, which has been successfully used in nonlinear system. Due to the complexity of implementation, FCRM has never been used in color image segmentation and was thus explored in this investigation. Furthermore, the lack of spatial information is one of the problems of fuzzy-based clustering algorithms for image segmentation [17]. In order to overcome the noise in images spatial information is integrated in our FCRM implementation. We adopt a similarity factor combined with local intensity and spatial information that is adapted from Chuang et al. [12].

The experiments conducted used 15 images that were taken from the Berkeley Segmentation Database. The FCRM was compared against two comparison algorithms (FCM and GK) for color image segmentation. Three validity indices have been used and MSE and PSNR were measured. The images were reconstructed using the grayscale level. The experimental results revealed that FCRM achieves better results in most cases than the other approaches based on the aforementioned measures.

As for future work, FCRM is similar to other fuzzy partition techniques; thus, cluster centroids and the number of clusters should be decided in advance. However, for most unknown environments, the appropriate and exact number of clusters is unknown in practice. A new cluster validity criterion needs to be developed to determine the appropriate number of clusters. In addition, FCRM is very sensitive to the initialization. A good initialization results in good quality image segmentation, while an unsuitable initialization returns poor results. Thus, in future, a new technique for

Figure 2: Original image, grayscale image using FCM, GK, and FCRM are listed, respectively.

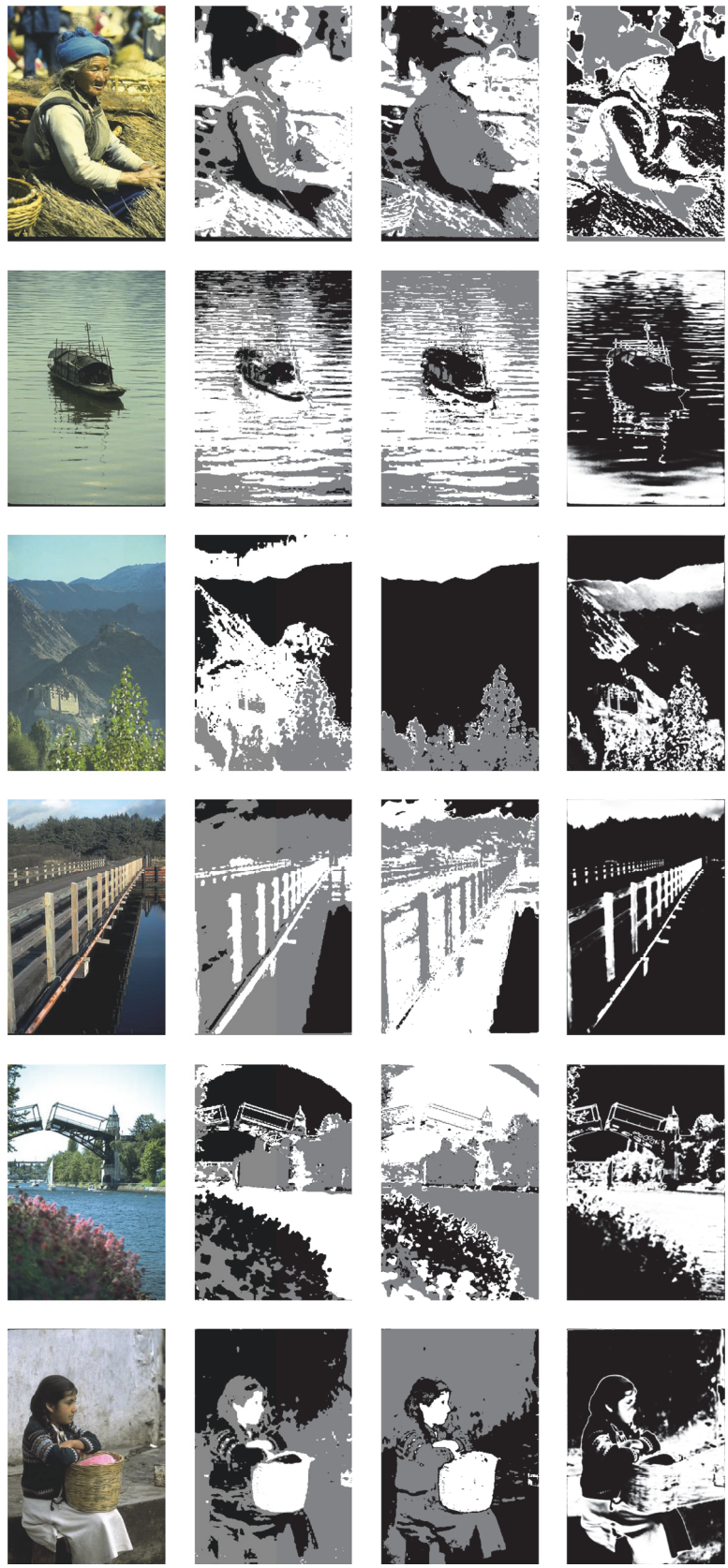

Figure 3: Original image, grayscale image using FCM, GK, and FCRM are listed, respectively (continued).

Table 12: PSNR using GK with different cluster number.

	$c = 2$	3	4	5	6	7	8	9	10
IMG1	10.47	11.88	13.18	14.05	14.51	15.01	15.93	16.39	17.12
IMG2	12.41	13.98	15.32	16.04	16.49	17.00	17.92	18.38	19.11
IMG3	9.14	10.77	12.07	13.09	13.55	14.06	14.98	15.43	16.17
IMG4	7.91	9.67	11.03	11.87	12.32	12.83	13.75	14.21	14.94
IMG5	12.22	13.93	15.06	16.12	16.57	17.08	18.00	18.46	19.19
IMG6	10.97	10.97	12.15	13.07	13.52	14.03	14.95	15.41	16.14
IMG7	12.00	13.83	13.48	14.19	14.64	15.15	16.07	16.53	17.26
IMG8	11.12	12.78	14.08	15.16	15.62	16.13	17.05	17.51	18.24
IMG9	8.21	9.92	11.13	12.12	12.58	13.08	14.01	14.46	15.20
IMG10	8.21	9.23	10.56	11.38	11.84	12.35	13.27	13.72	14.46
IMG11	8.44	10.23	11.43	12.36	12.81	13.32	14.24	14.70	15.43
IMG12	9.09	10.19	11.37	12.29	12.75	13.25	14.17	14.63	15.36
IMG13	9.76	11.88	12.79	13.83	14.29	14.80	15.72	16.18	16.91
IMG14	9.49	11.20	12.50	13.48	13.93	14.44	15.36	15.82	16.55
IMG15	10.43	12.07	13.42	14.12	14.57	15.08	16.00	16.46	17.19

Table 13: PSNR using FCRM with different cluster number.

	$c = 2$	3	4	5	6	7	8	9	10
IMG1	10.55	12.10	13.26	14.10	14.56	15.06	15.98	16.44	17.18
IMG2	12.44	14.12	15.30	16.23	16.69	17.19	18.11	18.57	19.30
IMG3	9.21	10.78	12.14	13.13	13.59	14.10	15.02	15.48	16.21
IMG4	8.97	10.19	11.13	11.89	12.35	12.85	13.77	14.23	14.96
IMG5	12.23	13.98	15.14	16.14	16.60	17.11	18.03	18.49	19.22
IMG6	11.29	11.70	12.91	13.61	14.07	14.58	15.50	15.95	16.69
IMG7	12.13	13.85	13.96	14.24	14.70	15.20	16.12	16.58	17.32
IMG8	11.16	12.70	14.19	15.21	15.67	16.17	17.09	17.55	18.28
IMG9	8.23	9.95	11.18	12.13	12.59	13.10	14.02	14.47	15.21
IMG10	8.35	9.31	10.70	11.68	12.13	12.64	13.56	14.02	14.75
IMG11	8.45	10.28	11.46	12.37	12.82	13.33	14.25	14.71	15.44
IMG12	9.18	10.71	10.96	11.89	12.35	12.85	13.77	14.23	14.96
IMG13	9.78	11.89	13.07	13.90	14.36	14.86	15.78	16.24	16.97
IMG14	9.50	11.48	12.51	14.27	14.73	15.24	16.16	16.62	17.35
IMG15	10.56	12.19	13.64	14.19	14.64	15.15	16.07	16.53	17.26

automatically finding the exact number of clusters as well as obtaining good initialization needs to be investigated.

Conflicts of Interest

The authors declare that they have no conflicts of interest.

References

[1] L. G. Shapiro and G. C. Stockman, *Computer Vision*, Prentice-Hall, Upper Saddle River, NJ, USA, 2002.

[2] D. L. Pham, C. Xu, and J. L. Prince, "Current methods in medical image segmentation," *Annual Review of Biomedical Engineering*, vol. 2, no. 2000, pp. 315–337, 2000.

[3] J. Malik, S. Belongie, T. Leung, and J. Shi, "Contour and texture analysis for image segmentation," *International Journal of Computer Vision*, vol. 43, no. 1, pp. 7–27, 2001.

[4] S. Krinidis and V. Chatzis, "A robust fuzzy local information C-means clustering algorithm," *IEEE Transactions on Image Processing*, vol. 19, no. 5, pp. 1328–1337, 2010.

[5] M. Sezgin and B. Sankur, "Survey over image thresholding techniques and quantitative performance evaluation," *Journal of Electronic Imaging*, vol. 13, no. 1, pp. 146–168, 2004.

[6] N. Senthilkumaran and R. Rajesh, "Edge detection techniques for image segmentation—a survey of soft computing approaches," *International Journal of Recent Trends in Engineering*, vol. 1, no. 2, 2009.

[7] K. Haris, S. N. Efstratiadis, N. Maglaveras, and A. K. Katsaggelos, "Hybrid image segmentation using watersheds and fast region merging," *IEEE Transactions on Image Processing*, vol. 7, no. 12, pp. 1684–1699, 1998.

[8] J. Fan, D. K. Y. Yau, A. K. Elmagarmid, and W. G. Aref, "Automatic image segmentation by integrating color-edge extraction and seeded region growing," *IEEE Transactions on Image Processing*, vol. 10, no. 10, pp. 1454–1466, 2001.

[9] T. Kasetkasem, M. K. Arora, and P. K. Varshney, "Super-resolution land cover mapping using a Markov random field based approach," *Remote Sensing of Environment*, vol. 96, no. 3-4, pp. 302–314, 2005.

[10] F. Amat, F. Moussavi, L. R. Comolli, G. Elidan, K. H. Downing, and M. Horowitz, "Markov random field based automatic image alignment for electron tomography," *Journal of Structural Biology*, vol. 161, no. 3, pp. 260–275, 2008.

[11] Z. Wu and R. Leahy, "An optimal graph theoretic approach to data clustering: theory and its application to image segmentation," *IEEE Transactions on Pattern Analysis and Machine Intelligence*, vol. 15, no. 11, pp. 1101–1113, 1993.

[12] K.-S. Chuang, H.-L. Tzeng, S. Chen, J. Wu, and T.-J. Chen, "Fuzzy c-means clustering with spatial information for image segmentation," *Computerized Medical Imaging and Graphics*, vol. 30, no. 1, pp. 9–15, 2006.

[13] N. R. Pal and S. K. Pal, "A review on image segmentation techniques," *Pattern Recognition*, vol. 26, no. 9, pp. 1277–1294, 1993.

[14] J. C. Bezdek, R. Ehrlich, and W. Full, "FCM: the fuzzy c-means clustering algorithm," *Computers and Geosciences*, vol. 10, no. 2-3, pp. 191–203, 1984.

[15] J. C. Bezdek, *Pattern Recognition with Fuzzy Objective Function Algorithms*, Plenum Press, New York, NY, USA, 1981.

[16] J. C. Bezdek, J. Keller, R. Krisnapuram, and N. R. Pal, *Fuzzy Models and Algorithms for Pattern Recognition and Image Processing*, vol. 4, Springer, New York, NY, USA, 1999.

[17] W. Cai, S. Chen, and D. Zhang, "Fast and robust fuzzy c-means clustering algorithms incorporating local information for image segmentation," *Pattern Recognition*, vol. 40, Article ID 825838, 2007.

[18] A. A. Othman and H. R. Tizhoosh, "Evolving fuzzy image segmentation," in *Proceedings of the IEEE International Conference on Fuzzy Systems (FUZZ '11)*, pp. 1603–1609, June 2011.

[19] Y. A. Tolias and S. M. Panas, "On applying spatial constraints in fuzzy image clustering using a fuzzy rule-based system," *IEEE Signal Processing Letters*, vol. 5, no. 10, pp. 245–247, 1998.

[20] G. Krell, H. R. Tizhoosh, T. Lilienblum, C. J. Moore, and B. Michaelis, "Enhancement and associative restoration of electronic portal images in radiotherapy," *International Journal of Medical Informatics*, vol. 49, no. 2, pp. 157–171, 1998.

[21] G. C. Karmakar and L. S. Dooley, "A generic fuzzy rule based image segmentation algorithm," *Pattern Recognition Letters*, vol. 23, no. 10, pp. 1215–1227, 2002.

[22] G. Karmakar, L. Dooley, and M. Murshed, "Fuzzy rule for image segmentation incorporating texture features," in *Proceedings of the International Conference on Image Processing (ICIP '02)*, pp. I/797–I/800, September 2002.

[23] S. K. Pal and A. Rosenfeld, "Image enhancement and thresholding by optimization of fuzzy compactness," *Pattern Recognition Letters*, vol. 7, no. 2, pp. 77–86, 1988.

[24] S. K. Pal and A. Ghosh, "Fuzzy geometry in image analysis," *Fuzzy Sets and Systems*, vol. 48, no. 1, pp. 23–40, 1992.

[25] V. V. Krivsha and S. A. Butenkov, "Classification using fuzzy geometric features," in *Proceedings of the IEEE International Conference on Artificial Intelligence Systems (ICAIS '02)*, pp. 89–91, September 2002.

[26] S. K. Pal, A. Ghosh, and B. Uma Shankar, "Segmentation of remotely sensed images with fuzzy thresholding, and quantitative evaluation," *International Journal of Remote Sensing*, vol. 21, no. 11, pp. 2269–2300, 2000.

[27] J. Noordam, W. van den Broek, and L. Buydens, "Geometrically guided fuzzy C-means clustering for multivariate image segmentation," in *Proceedings of the 15th International Conference on Pattern Recognition (ICPR '00)*, vol. 1, pp. 462–465, Barcelona, Spain, September 2000.

[28] D. Bhandari, N. R. Pal, and D. Dutta Majumder, "Fuzzy divergence, probability measure of fuzzy events and image thresholding," *Pattern Recognition Letters*, vol. 13, no. 12, pp. 857–867, 1992.

[29] C. A. Murthy and S. K. Pal, "Fuzzy thresholding: mathematical framework, bound functions and weighted moving average technique," *Pattern Recognition Letters*, vol. 11, no. 3, pp. 197–206, 1990.

[30] Q. Wang, Z. Chi, and R. Zhao, "Image thresholding by maximizing the index of nonfuzziness of the 2-D grayscale histogram," *Computer Vision and Image Understanding*, vol. 85, no. 2, pp. 100–116, 2002.

[31] E. Lughofer, "On-line evolving image classifiers and their application to surface inspection," *Image and Vision Computing*, vol. 28, no. 7, pp. 1065–1079, 2010.

[32] R. Rajesh, N. Senthilkumaran, J. Satheeshkumar, B. S. Priya, C. Thilagavathy, and K. Priya, "On the type-1 and type-2 fuzziness measures for thresholding MRI brain images," in *Proceedings of the IEEE International Conference on Fuzzy Systems (FUZZ '11)*, pp. 992–995, IEEE, Taipei, Taiwan, June 2011.

[33] D. R. Neog, M. A. Raza, and F. C.-H. Rhee, "An interval type 2 fuzzy approach to multilevel image segmentation," in *Proceedings of the IEEE International Conference on Fuzzy Systems (FUZZ '11)*, pp. 1164–1170, IEEE, June 2011.

[34] T. Chaira, "Accurate segmentation of leukocyte in blood cell images using Atanassov's intuitionistic fuzzy and interval Type II fuzzy set theory," *Micron*, vol. 61, pp. 1–8, 2014.

[35] L. Szilagyi, Z. Benyo, S. M. Szilagyi, and H. S. Adam, "MR brain image segmentation using an enhanced fuzzy C-means algorithm," in *Proceedings of the 25th Annual International Conference of the IEEE Engineering in Medicine and Biology Society*, vol. 1, pp. 724–726, IEEE, September 2003.

[36] M. Gong, Y. Liang, J. Shi, W. Ma, and J. Ma, "Fuzzy C-means clustering with local information and kernel metric for image segmentation," *IEEE Transactions on Image Processing*, vol. 22, no. 2, pp. 573–584, 2013.

[37] F. Zhao, L. Jiao, H. Liu, and X. Gao, "A novel fuzzy clustering algorithm with non local adaptive spatial constraint for image segmentation," *Signal Processing*, vol. 91, no. 4, pp. 988–999, 2011.

[38] Z. Ji, Y. Xia, Q. Chen, Q. Sun, D. Xia, and D. D. Feng, "Fuzzy c-means clustering with weighted image patch for image segmentation," *Applied Soft Computing*, vol. 12, no. 6, pp. 1659–1667, 2012.

[39] B. Sowmya and B. Sheela Rani, "Colour image segmentation using fuzzy clustering techniques and competitive neural network," *Applied Soft Computing Journal*, vol. 11, no. 3, pp. 3170–3178, 2011.

[40] K. S. Tan, W. H. Lim, and N. A. M. Isa, "Novel initialization scheme for Fuzzy C-Means algorithm on color image segmentation," *Applied Soft Computing Journal*, vol. 13, no. 4, pp. 1832–1852, 2013.

[41] K. Deshmukh and G. N. Shinde, "An adaptive neuro-fuzzy system for color image segmentation," *Journal of the Indian Institute of Science*, vol. 86, no. 5, pp. 493–506, 2006.

[42] F. A. Jassim, "Hybrid image segmentation using discerner cluster in FCM and histogram thresholding," *International Journal of Graphics and Image Processing*, vol. 2, no. 4, 2012.

[43] J. Liu and S. Qiao, "A image segmentation algorithm based on differential evolution particle swarm optimization fuzzy c-means clustering," *Computer Science and Information Systems*, vol. 12, no. 2, pp. 873–893, 2015.

[44] S.-L. Jui, C. Lin, H. Guan, A. Abraham, A. E. Hassanien, and K. Xiao, "Fuzzy c-means with wavelet filtration for MR image segmentation," in *Proceedings of the 6th World Congress on Nature and Biologically Inspired Computing (NaBIC '14)*, pp. 12–16, IEEE, Porto, Portugal, August 2014.

[45] Y. Yang and S. Huang, "Image segmentation by fuzzy C-means clustering algorithm with a novel penalty term," *Computing and Informatics*, vol. 26, no. 1, pp. 17–31, 2007.

[46] R. S. Hunter, "Photoelectric color-difference meter," *Journal of the Optical Society of America*, vol. 38, no. 7, p. 661, 1948, Proceedings of the Winter Meeting of the Optical Society of America.

[47] J. D. Foley, A. van Dam, S. K. Feiner, and J. F. Hughes, *Computer Graphics: Principles and Practice*, Addison-Wesley, Redwood City, Calif, USA, 2nd edition, 1995.

[48] R. S. Hunter, "Accuracy, precision, and stability of new photoelectric color-difference meter," *Journal of the Optical Society of America*, vol. 38, no. 12, p. 1094, 1948, Proceedings of the Thirty-Third Annual Meeting of the Optical Society of America.

[49] T. Takagi and M. Sugeno, "Fuzzy identification of systems and its applications to modeling and control," *IEEE Transactions on Systems, Man, and Cybernetics*, vol. 15, no. 1, pp. 116–132, 1985.

[50] J. C. Bezdek, C. Coray, R. Gunderson, and J. Watson, "Detection and characterization of cluster substructure II. Fuzzy c-varieties and convex combinations thereof," *SIAM Journal on Applied Mathematics*, vol. 40, no. 2, pp. 358–372, 1981.

[51] R. N. Dave, "Validating fuzzy partitions obtained through c-shells clustering," *Pattern Recognition Letters*, vol. 17, no. 6, pp. 613–623, 1996.

[52] M. Chen and S. A. Ludwig, "Fuzzy clustering using automatic particle swarm optimization," in *Proceedings of the IEEE International Conference on Fuzzy Systems (FUZZ-IEEE '14)*, pp. 1545–1552, IEEE, Beijing, China, July 2014.

[53] C. C. Fowlkes, D. R. Martin, and J. Malik, "Local figure-ground cues are valid for natural images," *Journal of Vision*, vol. 7, no. 8, article 2, 2007.

[54] K. McLaren, "Dyes, general survey," in *Ullmann's Encyclopedia of Industrial Chemistry*, Wiley-VCH, 2000.

[55] E. L. Lehmann and G. Casella, *Theory of Point Estimation*, Springer Texts in Statistics, Springer, New York, NY, USA, 2nd edition, 1998.

[56] Q. Huynh-Thu and M. Ghanbari, "Scope of validity of PSNR in image/video quality assessment," *Electronics Letters*, vol. 44, no. 13, pp. 800–801, 2008.